JCTC Journal of Chemical Theory and Computation

Reaction Ensemble Monte Carlo Simulation of Complex Molecular Systems

Thomas W. Rosch and Edward J. Maginn*

Department of Chemical and Biomolecular Engineering, University of Notre Dame, 182 Fitzpatrick Hall, Notre Dame, Indiana 46556-5637, United States

Received July 19, 2010

Abstract: Acceptance rules for reaction ensemble Monte Carlo (RxMC) simulations containing classically modeled atomistic degrees of freedom are derived for complex molecular systems where insertions and deletions are achieved gradually by utilizing the continuous fractional component (CFC) method. A self-consistent manner in which to utilize statistical mechanical data contained in ideal gas free energy parameters during RxMC moves is presented. The method is tested by applying it to two previously studied systems containing intramolecular degrees of freedom: the propene metathesis reaction and methyl-*tert*-butyl-ether (MTBE) synthesis. Quantitative agreement is found between the current results and those of Keil et al. (*J. Chem. Phys.* **2005**, *122*, 164705) for the propene metathesis reaction. Differences are observed between the equilibrium concentrations of the present study and those of Lísal et al. (*AIChE J.* **2000**, *46*, 866−875) for the MTBE reaction. It is shown that most of this difference can be attributed to an incorrect formulation of the Monte Carlo acceptance rule. Efficiency gains using CFC MC as opposed to single stage molecule insertions are presented.

1. Introduction

Techniques that rely on molecular simulation to investigate systems undergoing chemical reactions can be divided into two categories. One category, ab initio methods, relies on first principle calculations to rigorously calculate energy−structure relationships. Electronic degrees of freedom are captured in these methods, which allows for direct treatment of bond breaking, distortion, and formation. These methods work well for computing the equilibrium distribution of products in the gas phase. Incorporation into time-dependent algorithms, e.g., Car−Parrinello molecular dynamics (CP-MD),[1] allows reactions to be modeled directly, in principle. The accuracy of ab initio methods depends on the level of theory. Highly accurate methods scale poorly with system size, making them very difficult to apply to the condensed phase.[2] The second category of methods involves treating the interactions between atoms and molecules through classical potentials parametrized either from quantum mechanical calculations or experimental data. These methods alleviate the need to perform computationally expensive first principle calculations at each configuration, and thus much larger systems can be studied for longer periods of time. One approach is to use "reactive" force fields that are parametrized to treat chemical bond formation and breaking directly.[3−5] While application of these reactive potentials has led to significant insight into short-time transient behavior, to date there are relatively few systems for which parameters have been developed. It has also been found that these potentials are extremely sensitive to the way in which they were parametrized.[2] A comprehensive discussion of reactive force fields and their application can be found elsewhere.[6]

A second classically based approach is to ignore transient events, such as bond formation and breakage, and focus only on the equilibrium conversion of each species. Such an approach was independently developed by Smith and Triska[7] and Johnson et al.[8] within a Monte Carlo framework. The so-called reaction ensemble Monte Carlo (RxMC) method allows reactants and products to be interconverted through a series of stochastic moves. While there is no need for potentials containing parameters that describe bond formation and breakage, RxMC does require as input ideal gas free energy differences between species, which can be obtained

* Corresponding author. E-mail: ed@nd.edu.

10.1021/ct100615j
Published on Web 01/10/2011

either from thermophysical tables or quantum mechanical calculations. Also required is a specified reaction set describing the stoichiometry of the system and relevant intermolecular potentials that accurately describe interactions in the condensed phase. In practice, RxMC is similar to grand canonical Monte Carlo[9] (GCMC), because random insertion and deletion of molecular species (during forward and reverse reaction moves) propagate the system toward equilibrium. Reaction moves eliminate any activation barriers associated with transition states or molecular diffusion, thus achieving equilibrium concentrations in a wide number of highly nonideal systems irrespective of reaction rates. RxMC has been quite successful in predicting the equilibrium behavior of reactions for many systems. A comprehensive review of the method can be found elsewhere.[2]

Most applications of RxMC have focused on small molecules where internal degrees of freedom were constrained to equilibrium values.[7,8,10−14] For these systems, there is a clean separation between the classical and quantum mechanical contributions to the Monte Carlo acceptance rule (as shown in detail below). The situation is more complicated for systems where internal degrees of freedom cannot be constrained to their equilibrium values. Keil et al.[15,16] have formulated a set of RxMC acceptance rules for linear united atom alkanes and alkenes within a conventional configurational bias Monte Carlo (CBMC) framework. As shown previously,[17−19] this type of CBMC algorithm is only valid for models without coupling between bond angles, i.e., molecules without branch points. Lísal and co-workers have also modeled systems with flexible internal degrees of freedom within the RxMC framework.[20,21] Their system contained methyl-*tert*-butyl-ether (MTBE), a molecule with a flexible dihedral angle and coupling between bond angles. It is demonstrated below that this study did not properly incorporate these classical degrees of freedom with ideal gas quantum mechanical information within their Monte Carlo acceptance rules, which results in a shift in computed equilibrium concentrations.

One of the goals of the present work is to formulate a set of general acceptance rules for RxMC that self-consistently treats quantum mechanical and classical degrees of freedom for molecules of arbitrary complexity. A second objective is to show how a biasing strategy can be utilized with RxMC to improve sampling efficiency. Previous work by Lísal and co-workers has applied the expanded ensemble method to mesoscopic reaction ensemble dissipative dynamics simulations.[22,23] The focus of this work is on an adaptive slow growth method named continuous fractional component (CFC) Monte Carlo. The rest of this paper is organized as follows: In the next section background on RxMC is provided, and acceptance rules in this work are derived. Following this, derivation of the CFC method is provided followed by simulation details for two test cases. Next, results for the test cases are presented and compared with previous works. Finally a brief summary, and a set of conclusions are provided.

2. Methods

The reaction ensemble Monte Carlo method will be discussed for a system undergoing one reaction. It is straightforward to derive the method for multiple reactions in any number of phases. Equilibrium of a single reaction involving s species is reached when the following constraint is satisfied

$$\sum_{i=1}^{s} \nu_i \mu_i = 0 \tag{1}$$

where ν_i and μ_i are the stoichiometric coefficient and the chemical potential of species i, respectively. The Hamiltonian of each molecule is assumed to be separable into quantum and classical parts,[24] such that for a given species i

$$\mathscr{H}_i = \mathscr{H}_{i,\mathrm{qm}} + \mathscr{H}_{i,\mathrm{cl}} \tag{2}$$

where $\mathscr{H}_{i,\mathrm{cl}}$ is the Hamiltonian associated with the f_i degrees of freedom one wishes to treat classically, and $\mathscr{H}_{i,\mathrm{qm}}$ is the Hamiltonian associated with the remaining degrees of freedom that are treated quantum mechanically. During the simulation, only classical degrees of freedom will be allowed to change. Equation 2 implies that the molecular partition function is separable into quantum and classical components, such that the single molecule partition function is

$$q_i = q_{i,\mathrm{qm}} q_{i,\mathrm{cl}} = \frac{q_{i,\mathrm{qm}}}{\hbar^{f_i}} \int \exp[-\beta \mathscr{H}_{i,\mathrm{cl}}] \, \mathrm{d}p_i \, \mathrm{d}r_i \tag{3}$$

where $\hbar$ is Planck's constant, $\beta = 1/k_B T$, and p_i and r_i are the momenta and generalized coordinates associated with all the classical degrees of freedom of species i. Note that the molar standard chemical potential μ_i^0 is related to the total molecular partition function by

$$\frac{\mu_i^0}{RT} = -\ln\left(\frac{q_i}{\beta P^0 \Lambda_i^3}\right) \tag{4}$$

where P^0 is the standard state pressure and Λ is the de Broglie wavelength. The molar standard chemical potential can be obtained from thermochemical property databases[25,26] or computed from gas-phase quantum mechanical calculations and will be used as an input to the RxMC acceptance rules.

The semiclassical canonical partition function for a system containing a total of s species, each species i having N_i molecules, is

$$Q(N_1, \ldots, N_s, V, T) = \prod_{i=1}^{s} \frac{q_{i,\mathrm{qm}}^{N_i}}{N_i! \hbar^{f_i N_i}} \int \exp[-\beta \mathscr{H}_{\mathrm{cl}}] \, \mathrm{d}p \, \mathrm{d}r \tag{5}$$

where $\mathscr{H}_{\mathrm{cl}}$ is the classical Hamiltonian of the system with momenta and coordinates p and r, respectively. Equation 5 implies that all intermolecular interactions are treated classically. If the classical Hamiltonian is separable into potential and kinetic contributions, then the integration of momenta in eq 5 is straightforward. Moreover, if the classical potential only involves pairwise interactions and there are no external fields, then it is possible to integrate over the translational components of the generalized coordinates. The result is that

$$Q(N_1, \ldots, N_s, V, T) = \prod_{i=1}^{s} \frac{q_{i,\mathrm{qm}}^{N_i} V^{N_i}}{N_i! \Lambda_i^{f_i N_i}} \int \exp[-\beta \mathscr{V}_{\mathrm{cl}}] \, \mathrm{d}r' \tag{6}$$

where r' represents all the classical degrees of freedom minus translational terms and $\mathcal{V}'_{\mathrm{cl}}$ is the classical pairwise potential energy associated with the classical degrees of freedom.

The volume associated with the remaining classical degrees of freedom of a given species i will be given the symbol Ω_i, such that

$$\Omega_i = \int \mathrm{d}r'_i \tag{7}$$

It follows that the volume associated with *all* the classical degrees of freedom is

$$\Omega_i V = \int \mathrm{d}r_i \tag{8}$$

The grand ensemble is the most appropriate for RxMC, and the grand partition function can be written as the canonical partition function of eq 6, expanded in chemical potential:

$$\Xi(\mu_1, ..., \mu_s, V, T) = \sum_{N_1=0}^{\infty} \cdots \sum_{N_s=0}^{\infty} \int \exp\left[\beta \sum_{i=1}^{s} N_i \mu_i - \sum_{i=1}^{s} \ln N_i! + \sum_{i=1}^{s} N_i \ln \frac{V q_{i,\mathrm{qm}}}{\Lambda_i^{f_i}} - \beta \mathcal{V}\right] \mathrm{d}r' \tag{9}$$

where the subscript cl designating the potential as classical has been dropped for simplicity.

From eq 9, the probability of state m in the grand ensemble is

$$\rho_m = \frac{1}{\Xi(\mu_1, ..., \mu_s, V, T)} \exp\left[\beta \sum_{i=1}^{s} N_{i,m} \mu_i - \sum_{i=1}^{s} \ln N_{i,m}! + \sum_{i=1}^{s} N_{i,m} \ln\left(\frac{\Omega_i V q_{i,\mathrm{qm}}}{\Lambda_i^{f_i}}\right) - \beta \mathcal{V}'_m\right] \tag{10}$$

Note that the number of each species as well as the potential energy depend upon state m.

Equation 10 will be the basis for the derivation of acceptance rules in the RxMC method. The detailed balance condition requires that moves between states m and n satisfy the following expression:[27]

$$\prod_{mn} \alpha_{mn} \rho_m = \prod_{nm} \alpha_{nm} \rho_n \tag{11}$$

where Π_{mn} is the one-step transition probability of going from state m to state n, α_{mn} is underlying matrix of the Markov chain (the move "attempt" probability in going from state m to state n), and ρ_m is given by eq 10.

Within a RxMC simulation, transitions of the system from state m to n fall into two categories. One is for transitions where no change in species composition occurs, and the second is for a reaction move where the composition does change. Let the parameter δ differentiate between the three possible cases. When $\delta = 0$, no reaction occurs. When $\delta = +1$, a forward reaction occurs such that reactants (species with a negative stoichiometric coefficient) are consumed and products (species with a positive stoichiometric coefficient) are produced. For a reverse reaction that consumes products and produces reactants, $\delta = -1$. For any species i initially in state m with $N_{i,m}$ molecules, there will be $N_{i,n}$ molecules in the new state n given by

$$N_{i,n} = (N_{i,m} + \nu_i \delta) \tag{12}$$

Combining eqs 10−12 results in the following general formulation of the one-step transition probability for RxMC moves:

$$\Pi_{mn} = \min\left(1, \frac{\alpha_{nm}}{\alpha_{mn}}\left[\prod_{i=1}^{s} \frac{N_{i,m}!}{(N_{i,m} + \nu_i \delta)!}\left(\frac{\Omega_i V q_{i,\mathrm{qm}}}{\Lambda^{f_i}}\right)^{\nu_i \delta}\right] \times \exp[-\beta(\Delta \mathcal{V}_{mn}^{\mathrm{inter}} + \Delta \mathcal{V}_{mn}^{\mathrm{intra}})]\right) \tag{13}$$

where eq 1 has been employed, and the change in potential energy has been divided into classical intramolecular and intermolecular contributions $\Delta \mathcal{V}_{mn}^{\mathrm{intra}}$ and $\Delta \mathcal{V}_{mn}^{\mathrm{inter}}$, respectively. Note that the quantum molecular partition function $q_{i,\mathrm{qm}}$ appears in eq 13 and not the total molecular partition function q_i.

If molecules are treated as rigid such that intramolecular degrees of freedom are frozen at their equilibrium values, then only intermolecular and translational degrees of freedom are treated classically (i.e., $f_i = 3$). A molecule only adopts one conformation so $q_{i,\mathrm{qm}} = q_i$, $\Delta \mathcal{V}_{mn}^{\mathrm{intra}} = 0$, and $\Omega_i = 1$. Also, if no biasing is used, then the stochastic matrix is symmetric such that $\alpha_{mn} = \alpha_{nm}$. In this case, eq 13 reduces to the conventional acceptance rule used in many previous studies in which small, rigid molecules were simulated.[7,8,10−14]

When simulations are performed on more complex molecules that cannot be treated realistically as rigid, intramolecular conformations must be modeled subject to a classical intramolecular potential function, $\Delta \mathcal{V}_{mn}^{\mathrm{intra}}$. For example, $\Delta \mathcal{V}_{mn}^{\mathrm{intra}}$ may include terms that capture bond angle bending and dihedral angle rotation. In these cases, eq 13 must be used. One must be careful to properly account for the fact that $q_{i,\mathrm{qm}}$ and not q_i appears in the acceptance rules. For example, the use of tabulated values of μ_i^0 will lead to an incorrect accounting of the classical and quantum mechanical terms (see eq 4). Below it is shown how to formulate a set of self-consistent RxMC moves that satisfy eq 13 and still allow the use of q_i or μ_i^0 in the acceptance rule.

The approach relies upon the use of a "reservoir sampling" method to generate conformations of flexible molecules with a known probability. More details of the method as well as how it can be combined with configurational biasing is found elsewhere,[17] but for simplicity only the basic method is outlined below. To apply the method, molecules are broken into fragments. Each fragment contains atoms connected only by bond lengths and angles. These degrees of freedom can be classified as "hard" because they are very strong functions of position. Each fragment is connected to another via one dihedral potential, which is a weaker function of position compared to bond lengths or angles and is thus known as a "soft" degree of freedom. This method decouples "hard" and "soft" degrees of freedom and allows for a systematic approach to build molecules that satisfy a Boltzmann distribution of internal energy. A reservoir of each kind of fragment is created via a standard Metropolis Monte Carlo

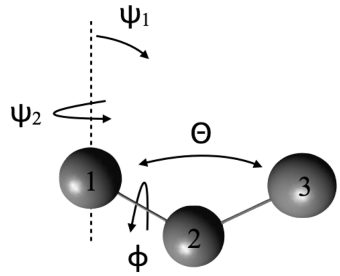

Figure 1. Internal coordinates associated with a particular three-atom fragment.

presimulation. Each fragment appears in the reservoir with a well-defined probability according to the Boltzmann weight of all the flexible degrees of freedom in that fragment. That is, the probability of a given fragment appearing in the reservoir is

$$\rho_{\text{frag}} = \frac{\exp[-\beta \mathcal{V}^{\text{frag}}]\Delta V_{\text{frag}}}{\sum_{n\text{frags}} \exp[-\beta \mathcal{V}^{\text{frag}}]\Delta V_{\text{frag}}} \approx \frac{\exp[-\beta \mathcal{V}^{\text{frag}}]\mathrm{d}V_{\text{frag}}}{\int \exp[-\beta \mathcal{V}^{\text{frag}}]\mathrm{d}V_{\text{frag}}} \tag{14}$$

where *n*frags is the number of fragments in the reservoir, $\mathcal{V}^{\text{frag}}$ is the classical potential energy of the fragment and ΔV_{frag} and $\mathrm{d}V_{\text{frag}}$ are the discrete and differential volume elements associated with the flexible classical degrees of freedom of the fragment, minus the center of mass. For example, a three-atom fragment with fixed bond lengths but a flexible bond angle, such as the one shown in Figure 1, has associated with it the translational volume of atom 1 ($\mathrm{d}V_1 = \mathrm{d}x_1\mathrm{d}y_1\mathrm{d}z_1$) and the internal coordinate volume terms. Atom 2 is specified by two Euler angles Ψ_1 and Ψ_2 as well as a Jacobian associated with Ψ_1

$$\mathrm{d}V_2 = \mathrm{d}\cos(\Psi_1)\mathrm{d}\Psi_2 = 4\pi \tag{15}$$

and for atom 3 the differential volume element is

$$\mathrm{d}V_3 = \mathrm{d}\cos(\theta)\mathrm{d}\phi = 4\pi \tag{16}$$

So in this particular case, $\mathrm{d}V_{\text{frag}} = \mathrm{d}V_2\mathrm{d}V_3$.

Each fragment required to assemble a molecule is chosen according to eq 14 and connected to one another through one bond. As will be shown below, the dihedral angle ϕ that defines the relative orientation of two fragments is chosen according to

$$\rho_\phi = \frac{\exp[-\beta \mathcal{V}'_\phi]\Delta V_\phi}{\sum \exp[-\beta \mathcal{V}'_\phi]\Delta V_\phi} \approx \frac{\exp[-\beta \mathcal{V}'_\phi]\mathrm{d}V_\phi}{\int \exp[-\beta \mathcal{V}'_\phi]\mathrm{d}V_\phi} \tag{17}$$

where $\mathcal{V}'_\phi$ contains all the energy associated with dihedral angle ϕ and any nonbonded intramolecular energy interactions between the fragments involved in the dihedral angle. For simple molecules that do not contain nonbonded intramolecular interactions, a simple rejection method prevalent in configurational bias techniques may be used to generate the correct dihedral distribution. For more complex topologies that contain nonbonded terms, a number of methods may be utilized, e.g., presimulations of single molecules in the ideal gas phase which tabulate dihedral probability functions.

Once the entire molecule is assembled, the probability of a particular conformation for a molecule *i* being inserted into the system is

$$\rho_{\text{ins},i} = \frac{\mathrm{d}V_{com}}{V} \prod_{j=1}^{n\text{frags}} \rho_{\text{frag},j}\rho_{\phi,j} \tag{18}$$

where $\mathrm{d}V_{\text{com}}/V$ accounts for the random insertion of the center of mass of the molecule. Note that

$$\mathrm{d}r' = \prod_{j=1}^{n\text{frags}} \mathrm{d}V_{\text{frag},j}\,\mathrm{d}V_{\phi,j} \tag{19}$$

When a molecule is deleted from the system, no energy bias is used. Thus the probability of a configuration of deleted species *i* is

$$\rho_{\text{del},i} = \frac{\mathrm{d}V_{\text{com}}}{V}\frac{\mathrm{d}r'_i}{\Omega_i} \tag{20}$$

The underlying Markov matrix of insertion and deletion moves can be constructed from eqs 18 and 20. The ratio of attempt probabilities is

$$\frac{\alpha_{nm}}{\alpha_{mn}} = \prod_{i=1}^{s}\left[\left(\frac{\int \exp[-\beta \mathcal{V}_i^{\text{intra}}]\mathrm{d}r'_i}{\exp[-\beta \mathcal{V}_i^{\text{intra}}]\mathrm{d}r'_i}\right)\left(\frac{\mathrm{d}r'_i}{\Omega_i}\right)\right]^{\nu_i\delta} \tag{21}$$

Since the single molecule classical partition function is

$$q_{i,\text{cl}} = \frac{V}{\Lambda^{f_i}}\int \exp[-\beta \mathcal{V}_i^{\text{intra}}]\mathrm{d}r'_i \tag{22}$$

Equation 21 becomes

$$\frac{\alpha_{nm}}{\alpha_{mn}} = \prod_{i=1}^{s}\left[\left(\frac{\Lambda^{f_i}q_{i,\text{cl}}}{\mathrm{d}r'_i V \exp[-\beta \mathcal{V}_i^{\text{intra}}]}\right)\frac{\mathrm{d}r'_i}{\Omega_i}\right]^{\nu_i\delta} \tag{23}$$

Finally, substituting eq 23 into 13, the desired result for the one-step transition probability is obtained

$$\Pi_{mn} = \min\left(1, \prod_{i=1}^{s}\left[\frac{N_{i,m}!}{(N_{i,m}+\nu\delta)!}q_i^{\nu_i\delta}\right]\exp[-\beta(\Delta \mathcal{V}_{mn}^{\text{inter}})]\right) \tag{24}$$

Note that the full single molecule partition function appears in the acceptance rule and that only the difference in intermolecular classical potential energy is used. By definition the conformations used in reaction moves already satisfy a Boltzmann distribution in regards to their intramolecular energy, and thus only intermolecular terms appear in eq 24. This acceptance rule is convenient to use because it allows one to use standard thermochemical data for the ideal gas partition function of the molecule. Note that in the absence of any intermolecular interactions, the ideal gas ratio of free energies completely determines the equilibrium concentrations of the reacting mixture, as is required. Intramolecular conformations will also appear according to an ideal gas

probability distribution since eq 23 was used. Equation 24 is the main result, but it must be emphasized that it is valid only if one generates configurations consistent with eq 23.

As mentioned in the Introduction, Lísal and co-workers modeled the MTBE synthesis reaction. MTBE contains three flexible dihedral angles that are modeled using a classical potential. From private communications with the authors, it was ascertained that they generated random configurations for MTBE such that $\alpha_{mn} = \alpha_{nm}$. To ensure that intramolecular degrees of freedom were properly sampled, the intramolecular potential energy was included in the acceptance rule. They also used the molar standard chemical potential which is related to the full molecular partition function q_i through eq 4. Thus during a reaction move, their acceptance rule was

$$\Pi_{mn,\mathrm{Lisal}} = \min\left(1, \prod_{i=1}^{s}\left[\frac{N_i^m!}{(N_i^m + \nu_i\delta)!}q_i^{\nu_i\delta}\right] \times \exp[-\beta(\Delta\mathcal{V}_{mn}^{\mathrm{inter}} + \Delta\mathcal{V}_{mn}^{\mathrm{intra}})]\right) \quad (25)$$

It is clear from eq 25 that the intramolecular contribution is counted twice; once in the full molecular partition function q_i and once in the exponential term ($\Delta\mathcal{V}_{mn}^{\mathrm{intra}}$). If one considers the simple case of an ideal gas reaction in which components contain flexible intramolecular degrees of freedom, then the acceptance probability consistent with quantum mechanics is $\Pi_{mn,\,\mathrm{Lisal}} = \min(1, \prod_{i=1}^{s}[N_i^m!/((N_i^m + \nu_i\delta)!)q_i^{\nu_i\delta}])$. Equation 25 does not reduce to this, while eq 24 does. We will show explicit simulation results supporting this claim below.

The only other atomistically detailed RxMC study the authors are aware of involving flexible intramolecular degrees of freedom was carried out by Keil and co-workers. They derived acceptance rules for RxMC within a CBMC framework to study propene metathesis within confined environments.[15,16] While their formulation is only valid for linear molecules, it is consistent with the acceptance rules given in the present work. In particular, it is easy to show that eq A11 of their work[16] reduces to eq 23 if only one trial position of inserted molecules is attempted. Results from simulations testing eqs 23 and 25 for MTBE synthesis and propene metathesis are given in the next section.

Finally, the reservoir sampling method[17] is directly suited to include configurational bias in the RxMC framework, similar to that proposed by Keil and co-workers. An alternative method to CBMC, described below, relies on slow growth to overcome large free energy barriers associated with insertion and deletion in dense fluids. In the continuous fractional component (CFC) MC method,[28] insertions and deletions are not accomplished in one step but rather by gradual changes in the intermolecular coupling of fractional molecules to the rest of the system. The coupling of the fractional molecules is controlled by a parameter λ that fluctuates between 0 and 1. At $\lambda = 0$ the reactant molecules have no intermolecular interaction with the system, while the product molecules are completely coupled to the system. At $\lambda = 1$ the opposite is true; product molecules are decoupled, while reactant molecules fully interact with the system. Regardless of the value of λ, the fractional molecules contain full intramolecular interactions (bond, angle, dihedral, improper, etc.). There is need only to define one λ associated with the reaction. Any species with a negative ν_i (reactant) will have a coupling parameter of λ, while any species with a positive ν_i (product) will have a coupling parameter of $1 - \lambda$. A major strength of slow-growth methods is their ability to incorporate a biasing function to aid in the transition through λ states. A biasing function $\eta(\lambda_j)$ that depends only on the amount of coupling between the system and the fractional molecules is used here. The semiclassical partition function for systems containing partially coupled molecules is found elsewhere.[28]

Reaction moves within a CFC framework are now replaced by moves from state m to n that consist of attempts to randomly alter the value of λ. A transition to state n where the value of the coupling parameter λ changes by an amount ξ will fall into either of two categories. The first category occurs if $0 \le (\lambda + \xi) \le 1$. In this category no addition and deletion of molecules occur, and the transition probability is

$$\prod_{mn,\lambda}^{1} = \min[1, \exp(-\beta\Delta\mathcal{V}_{mn}^{\mathrm{inter}})\exp(\eta(\lambda_n) - \eta(\lambda_m))] \quad (26)$$

Because there is no change in intramolecular energy for this category, the difference in energy in eq 26 is purely intermolecular. The biasing factors $\eta(\lambda_j)$ help overcome energy barriers and more efficiently sample λ space. Optimization of the weighting factors was done using the Wang−Landau method.[29]

The second category of λ transitions occurs if either $(\lambda + \xi) < 0$ or $(\lambda + \xi) > 1$. The former case $(\lambda + \xi < 0)$ refers to a "forward" reaction, while the latter $(\lambda + \xi > 1)$ is a "reverse" reaction. For a reverse reaction, coupling parameters of fractional reactant and product molecules are set to 1 and 0, respectively. Additionally new fractional reactant molecules are inserted into the system with a coupling parameter of $\lambda_{\mathrm{new}} = (\lambda + \xi) - 1$. Finally, random product molecules are selected from the system and their coupling parameter is set to $1 - \lambda_{\mathrm{new}}$. For a forward reaction, the coupling parameters of fractional product and reactant molecules are set to 1 and 0, respectively. New fractional reactant molecules are chosen from the system, and the coupling parameter is set to $\lambda_{\mathrm{new}} = (\lambda + \xi) + 1$. Finally, product molecules are inserted into the system with a coupling parameter of $1 - \lambda_{\mathrm{new}}$. The transition probability is very similar to that in eq 24, except that biasing values are included

$$\Pi_{mn,\lambda}^{2} = \min\left[1, \prod_{i=1}^{s}\left(\frac{N_i^m!}{(N_i^m + \nu_i\delta)!}q_i^{\nu_i\delta}\right) \times \exp(-\beta\Delta\mathcal{V}_{mn}^{\mathrm{inter}})\exp(\eta(\lambda_n) - \eta(\lambda_m))\right] \quad (27)$$

3. Simulation Details

3.1. Continuous Fractional Component Method. For simulations using the CFC MC method, a scaled potential[28]

was used to model intermolecular interactions involving fractional molecules. For Lennard-Jones (LJ) interactions the following potential was used

$$\mathcal{V}_f = \lambda_{ij} 4\varepsilon_{ij} \left\{ \frac{1}{\left[\tau(1-\lambda_{ij})^2 + \left(\frac{r_{ij}}{\sigma_{ij}}\right)^6\right]^2} - \frac{1}{\left[\tau(1-\lambda_{ij})^2 + \left(\frac{r_{ij}}{\sigma_{ij}}\right)^6\right]} \right\} \quad (28)$$

λ_{ij} was taken to be the product of the scaling parameter of each molecule, $\lambda_{ij} = \lambda_i \times \lambda_j$, and τ is an adjustable parameter that was set to 0.5 following the work of Shi and Maginn.[28] Eq 28 shows that the full LJ potential is recovered at $\lambda_{ij} = 1$. For electrostatics, the partial charges on fractional molecules were scaled as $Q_f = \lambda_i^5 Q_i$ because nonlinear scaling is known to moderate strong electrostatic interactions resulting from insertion.[28]

As described in the Methods Section, bias factors were used to help push through free energy barriers associated with insertion or deletion in a dense system. Ideally the bias factors would allow any value of the scaling parameter λ to be sampled with equal probability. Recall that the scaling parameters of reactants (λ) and products ($1 - \lambda$) are not independent, thus a bias function $\eta(\lambda_j)$ dependent only upon the coupling of reactants is defined. The Wang−Landau method[29] was found to be efficient for determining $\eta(\lambda_j)$.[28] In practice λ was divided into 10 equal intervals, [0, 0.1), [0.1, 0.2), ..., [0.9, 1], with each interval j assigned a bias factor $\eta(\lambda_j)$. Initially all bias factors were set to 0. During equilibration, after an attempt to change λ, the value of $\eta(\lambda_j)$ was modified according to

$$\eta(\lambda_j) = \eta(\lambda_j) - \upsilon \quad (29)$$

where υ is a scaling parameter, initially set to 0.01. A histogram was kept that tracked the number of times each λ interval was visited. After 10 000 attempts to change the value of λ, the histogram was checked to see if each interval was visited at least 30% as often as the most visited interval. If this criterion was satisfied, then the scaling parameter was modified according to $\upsilon = 0.5\upsilon$, and histograms were reset to 0. Once the value of υ was equal to 5×10^{-6}, $\eta(\lambda_j)$ was no longer altered.

Subsequent λ moves perturb the same molecule until that molecule becomes either fully coupled or decoupled from the simulation box. Local relaxation around this molecule is thus critical for proper and efficient sampling. Preferential sampling, introduced by Owicki,[30] was utilized so that thermal equilibration moves were attempted more often for molecules surrounding the fractional ones. Two parameters are needed for preferential sampling, the volume around a fractional molecule V_{in} in which to bias thermal equilibration moves, and a parameter that governs the percentage of thermal equilibration moves to perform within that given volume $\hat{p}$. In the present work, $V_{in} = 4/3\pi(8\ \text{Å})^3$ and $\hat{p} =$ 85%, yielding ∼50% thermal moves attempted within the preferential volume.

3.2. MTBE Synthesis. To test the present method, two different systems were studied. One was the production of MTBE from isobutene and methanol, previously studied by Lísal and co-workers.[20,21] The reaction is given by

$$C_4H_8 + CH_3OH \leftrightarrow C_5H_{12}O \quad (30)$$

This system was chosen because it is one of only two cases where RxMC has been used in the condensed phase for flexible molecules. One objective was to test how the disparity between eqs 23 and 25 affect equilibrium concentrations of reactant and products. A second objective was to compare the efficiency of the CFC MC method relative to unbiased approaches. Isobutene and methanol were modeled using a united-atom version of the "optimized potentials for liquid simulations" (OPLS) model and contained no intramolecular degrees of freedom. MTBE was also modeled using OPLS, yet it has three flexible dihedral angles. Published potential parameters[21] were used with two exceptions. First, private correspondence with the authors revealed that the σ parameter for oxygen in MTBE used in their study was 3.0 Å, not 3.8 Å as reported. Second, Lísal and co-workers treated Coulombic long-range interactions by the reaction-field method, while the Ewald summation approach[31] was used here.

All MC simulations were conducted in the isothermal−isobaric (NPT) ensemble at 360 K and 5 bar. Each simulation was initialized with 512 molecules of various methanol to isobutene ratios. Geometric mixing rules were used to calculate ε_{ij} and σ_{ij} in eq 28. The cutoff distance r_{cut} for both the LJ and real space Coulombic interactions was set to 16 Å for the condensed phase and $65 \le r_{cut} \le 75$ Å for the vapor phase. LJ long-range corrections were added to the configurational energy assuming that the radial distribution function equaled unity beyond the cutoff.[27] Ewald parameters αL and K_{max} were set to 7.0 and 7.0, respectively, for both phases. Equilibrium simulations were run for 20×10^6 MC steps, and the standard deviation of four independent production runs of 20×10^6 MC steps was taken to be the statistical uncertainty. Translations, rotations about an axis, volume changes, intramolecular rearrangements, and reaction moves were attempted with probabilities of 20, 59.9, 0.1, 10, and 10%, respectively, for simulations absent gradual insertions and deletions. For simulations utilizing the CFC MC method, translations, rotations, volume changes, intramolecular rearrangements, and λ changes were attempted with probabilities of 35, 53.9, 0.1, 10, and 1%, respectively. All simulations were performed on dual core Intel opteron processors. The 80×10^6 MC steps required 1.5 days to complete.

3.3. Propene Metathesis. The RxMC method developed in this work was also applied to a system containing multiple reactions. Propene metathesis, studied by Keil and co-workers,[15] contains the following reactions

$$2C_3H_6 \leftrightarrow C_2H_4 + \text{trans} - C_4H_8 \quad (31)$$

Table 1. Single-Phase Vapor−Liquid Equilibrium Data Computed From Gibbs Ensemble Simulations[a]

T	P^{sat}_{LSN}	P^{sat}_{RM}	phase	$\mathscr{V}_{LSN}$	$\mathscr{V}_{RM}$	V_{LSN}	V_{RM}
				Isobutene			
350	10.51_{88}	10.32_{32}	g	-1.11_{11}	-1.09_{4}	2266_{225}	2332_{96}
			l	-15.47_{18}	-15.47_{4}	111.5_{13}	111.5_{3}
320	5.13_{50}	5.21_{36}	g	-0.59_{7}	-0.60_{4}	4635_{514}	4602_{353}
			l	-16.89_{16}	-16.88_{4}	103.7_{9}	103.8_{3}
				Methanol			
450	24.07_{267}	21.53_{88}	g	-5.94_{57}	-6.22_{37}	660.8_{388}	774.0_{437}
			l	-21.39_{69}	-24.06_{9}	66.18_{365}	59.22_{68}
420	13.23_{208}	15.78_{68}	g	-5.02_{61}	-4.46_{33}	1184_{95}	1636_{46}
			l	-24.95_{33}	-26.90_{4}	54.78_{106}	52.89_{8}
				MTBE			
480	19.26_{100}	20.65_{70}	g	-2.79_{21}	-0.94_{23}	1465_{105}	1309_{101}
			l	-17.55_{36}	-15.64_{16}	170.4_{34}	167.5_{16}
440	10.08_{37}	10.61_{26}	g	-1.43_{21}	0.36_{4}	2932_{364}	2790_{47}
			l	-20.27_{27}	-18.34_{2}	150.5_{19}	150.0_{2}

[a] $\mathscr{V}$, V, P^{sat} is the potential energy in kJ/mol, molar volume in cm^3/mol, and saturated vapor pressure in bar, respectively. Subscripts LSN and RM correspond to the work of Lísal et al. and the present work, respectively. Temperatures are in Kelvin.

$$2C_3H_6 \leftrightarrow C_2H_4 + \text{cis} - C_4H_8 \quad (32)$$

$$\text{cis} - C_4H_8 \leftrightarrow \text{trans} - C_4H_8 \quad (33)$$

Only two of these reactions are independent, and therefore eq 32 was not sampled during the simulation. The species involved in the propene metathesis were modeled using the TraPPE-UA model for inter- and intramolecular interactions. The parameters can be found elsewhere.[32,33]

NPT MC simulations were performed at 5 bar and temperatures of 300, 450, and 600 K. Lorentz−Berthelot combining rules were used to calculate ε_{ij} and σ_{ij} in eq 28. LJ long-ranged interactions were added to the configurational energy for a cutoff of $r_{cut} = 80$ Å. All simulations were initialized with 800 propene molecules. Equilibrium and production runs were conducted for the same number of steps as the MTBE system. Simulations required around 1 day to complete on dual core Intel opteron processors. Because this reaction occurs in the gas phase, the CFC MC method was not used; only single stage insertion and deletions were needed. Move attempt probabilities matched that for integer insertions and deletions in the MTBE system.

4. Results and Discussion

To determine what effect, if any, calculating long-ranged electrostatic interactions via the Ewald summation method rather than the reaction field method, the Gibbs ensemble MC simulations were conducted to compute pure component vapor−liquid equilibrium. Table 1 displays the comparison between this work and that reported by Lísal et al. Isobutene equilibrium bulk properties of this work agree with that of Lísal et al. to a high statistical precision. Interestingly, the properties of methanol and MTBE agree less perfectly, although in general the results are similar. Given that the methanol and MTBE models have partial charges while the isobutene model does not, the differences may be due to the fact that Lísal et al. used the reaction field method for calculating long-ranged electrostatics, while the Ewald summation method is used in the current work. Overall the agreement of single-component bulk properties is sufficient to proceed with comparison of the reaction ensemble method.

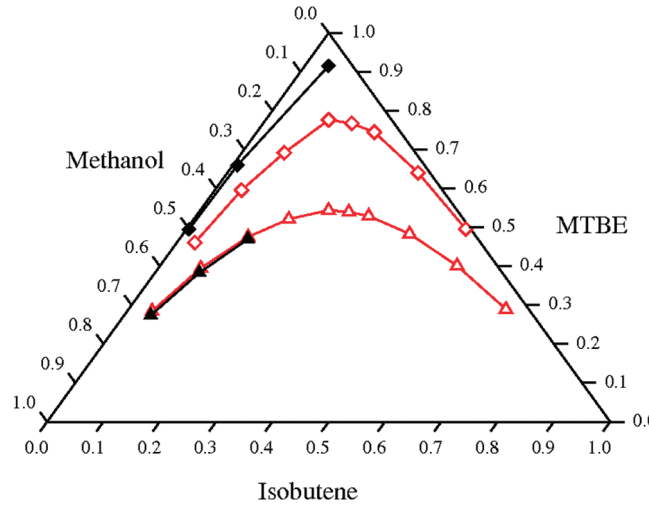

Figure 2. Triangular composition simplex for MTBE synthesis at $T = 360$ K and $P = 5$ bar. Diamonds and triangles correspond to liquid- and vapor-phase equilibrium compositions, respectively. Open symbols correspond to the work of Lísal et al.,[20] and filled symbols correspond to this work.

RxMC simulations were performed for three different initial mol ratios r of isobutene to methanol in both the gas and liquid phase at 360 K and 5 bar. Equilibrium properties were calculated in the vapor phase for $r = 0.34$, 0.51, and 0.67 and in the liquid phase for $r = 0.51$, 0.67, and 1.0. Data were first collected using single-step insertions and deletions using eq 24. A comparison of the present work with that of Lísal et al. is shown in Figure 2. Immediately apparent in the figure is how the environment affects reaction equilibria. The presence of intermolecular interactions in the condensed phase that are not found in the vapor phase shifts the reaction toward the right, resulting in more MTBE and less isobutene and methanol at equilibrium. Equilibrium compositions for the vapor phase obtained in the present study are in close agreement with the work of Lísal and co-workers, but there is a noticeable discrepancy in data for the liquid phase.

To probe the discrepancy between the liquid equilibrium composition predicted using eq 24 and that of Lísal et al., additional simulations were carried out at the same conditions in Figure 2 but using the acceptance rule of eq 25. Table 2 contains these results. Using eq 25 as the acceptance rule for a reaction move, condensed phase equilibrium mole fractions closely match the values reported by Lísal et al. However, both the liquid molar volume and vapor phase mole fractions match less well with the values of Lísal et al. Discrepancies may be due to differences in the treatment of electrostatic long-range corrections; the present work uses the Ewald summation technique, while Lísal et al. utilized the reaction field method. As this is the only difference in the method to calculate the data of the present work and that of Lísal et al., it would appear to be fortuitous that the current vapor-phase reaction results calculated using eq 24 matches the data of Lísal and co-workers. Regardless, the differences in equilibrium concentrations calculated using

Table 2. Vapor- and Liquid-Phase Equilibrium Properties for the MTBE Synthesis Reaction at $T = 360$ K and $P = 5$ bar[a]

		isobutene + methanol ↔ MTBE					
	$r =$	0.337	0.503		0.671		1.0
acc. rule	phase	gas	gas	liquid	gas	liquid	liquid
eq 24	z^1_{RM}	0.0473_{17}	0.0787_{9}	0.0045_{8}	0.1217_{37}	0.0082_{7}	0.0423_{13}
eq 25	z^1_{LSN}	0.044_{21}	0.0752_{28}	0.0319_{87}	0.1193_{47}	0.0475_{104}	0.1119_{145}
eq 25	z^1_{RM}	0.1256_{28}	0.1943_{22}	0.0232_{50}	0.2569_{39}	0.0386_{40}	0.1042_{18}
eq 24	z^2_{RM}	0.6791_{6}	0.5380_{5}	0.5008_{4}	0.4087_{25}	0.3323_{5}	0.0423_{13}
eq 25	z^2_{LSN}	0.6714_{7}	0.5295_{14}	0.5074_{44}	0.4053_{32}	0.3568_{70}	0.1119_{145}
eq 25	z^2_{RM}	0.7055_{9}	0.5959_{11}	0.5102_{25}	0.4998_{26}	0.3528_{27}	0.1042_{18}
eq 24	z^3_{RM}	0.2736_{23}	0.3833_{14}	0.4947_{12}	0.4696_{63}	0.6595_{12}	0.9153_{27}
eq 25	z^3_{LSN}	0.2846_{28}	0.3953_{42}	0.4607_{132}	0.4754_{78}	0.5957_{174}	0.7762_{290}
eq 25	z^3_{RM}	0.1689_{37}	0.2099_{33}	0.4666_{74}	0.2433_{64}	0.6086_{67}	0.7915_{36}
eq 24	$\mathscr{V}_{RM}$	-2.07_{37}	-1.64_{11}	-28.58_{12}	-0.61_{6}	-28.01_{3}	-27.32_{21}
eq 25	$\mathscr{V}_{LSN}$	-2.22_{34}	-1.57_{24}	-26.72_{51}	-1.31_{16}	-23.36_{39}	-23.67_{35}
eq 25	$\mathscr{V}_{RM}$	-2.62_{18}	-1.59_{9}	-28.10_{17}	-1.11_{9}	-27.36_{28}	-25.96_{3}
eq 24	V_{RM}	5802_{107}	5508_{35}	82.87_{28}	5684_{308}	95.00_{8}	115.2_{2}
eq 25	V_{LSN}	5152_{243}	5209_{258}	87.06_{144}	5413_{290}	99.04_{14}	117.4_{15}
eq 25	V_{RM}	4835_{170}	5388_{103}	82.12_{26}	5313_{247}	93.19_{43}	110.3_{2}

[a] Acc. rule, z^i, $\mathscr{V}$, and V correspond to the acceptance rule used, equilibrium mol fraction, molar volume, potential energy, and molar volume, respectively. Subscripts and units are the same as in Table 1.

eqs 24 and 25 clearly demonstrate the importance of a correct formulation of the acceptance rule.

To validate the equilibrium molar concentrations calculated in the present work using eq 24, satisfaction of eq 1 was tested. The total chemical potential is given by

$$\mu_i^{tot} = -k_B T \ln\left(\frac{q_i V}{\Lambda_i^3 N}\right) + \mu_i^{ex} \tag{34}$$

where μ_i^{ex} is the excess chemical potential of species i. The MTBE synthesis reaction is of the form A + B ↔ C, therefore a residual value R was defined

$$\mu_C^{tot} - \mu_B^{tot} - \mu_A^{tot} = R \tag{35}$$

Equation 34 inserted into eq 35 yields

$$-k_B T \ln\left(\frac{\dfrac{\beta P^0 V}{(N_C+1)}}{\dfrac{\beta P^0 V}{(N_B+1)}\dfrac{\beta P^0 V}{(N_A+1)}} K^0\right) + \mu_C^{ex} - \mu_B^{ex} - \mu_A^{ex} = R \tag{36}$$

where $P^0 = 1.0$ atm is the standard state pressure and $K^0 = 1.9823$ is the ideal gas equilibrium constant at 360 K. The ideal gas equilibrium constant is related to molecular partition functions through eq 4 and the following equation:

$$K^0 = \exp\left(-\frac{\sum_{i=1}^{s} \nu_i \mu_i^0}{RT}\right) \tag{37}$$

The residual in eq 36 was computed at equilibrium compositions resulting both from using eq 24 as well as eq 25 for two initial conditions: $r = 0.34$ in the vapor phase and $r = 1.0$ in the condensed phase. Values for these calculations are reported in Table 3. In the gas phase, the excess chemical potential of each species was computed using the Widom insertion method.[31] In condensed phases the Widom insertion method is known to be inefficient and at times incorrect.[34] Therefore an expanded ensemble method was used in this case.[35,36] During an RxMC simulation, 1000 equilibrium snapshots of the vapor phase were collected. Postsimulation, four independent sets of Widom insertions were performed. An independent set consisted of 1×10^5 insertions for each snapshot of the system. To calculate excess chemical potentials in the liquid-phase, four independent expanded ensemble simulations were performed for each species at the compositions of interest. Each simulation contained 15 subensembles and was run for 80×10^6 MC steps. The residuals corresponding to use of eq 24 in both vapor and liquid phases are 0 to within error, indicating that the system is in chemical equilibrium. The residuals corresponding to compositions using eq 25 statistically deviate from 0, which strengthens the argument that eq 25 is not formulated in a correct and self-consistent manner.

Table 3. Equilibrium Chemical Potentials for the Compositions of RM and LSN[a]

	isobutene(A)	methanol(B)	MTBE(C)	prefactor	R
		$r = 0.337$			
eq 24	-0.12_{1}	-0.31_{2}	-0.26_{1}	-0.28_{26}	-0.11_{26}
eq 25	-0.12_{1}	-0.39_{8}	-0.26_{1}	-1.88_{5}	-1.64_{9}
		$r = 1.0$			
eq 24	-2.11_{16}	-2.66_{4}	-4.88_{18}	-0.10_{1}	-0.21_{25}
eq 25	-3.07_{13}	-3.56_{19}	-6.33_{18}	-2.26_{1}	-1.97_{30}

[a] Each column has units of $k_B T$. The column labeled "prefactor" corresponds to the first term in eq 36.

To clear up any lingering doubts in the current method, a system devoid of any electrostatics interactions that contains intramolecular degrees of freedom was examined. Keil and co-workers[15,16] modeled propene metathesis using TraPPE-UA force fields where atomic degrees of freedom are encapsulated classically through angle and dihedral energy terms. The authors formulated acceptance rules in a similar manner to the present work to be used with configurational bias techniques and were able to reproduce experimental results with high accuracy. Conversion of propene to *cis*-butene, *trans*-butene, and ethene in bulk gas at 300, 450, and 600 K and 5 bar of pressure was calculated. The results

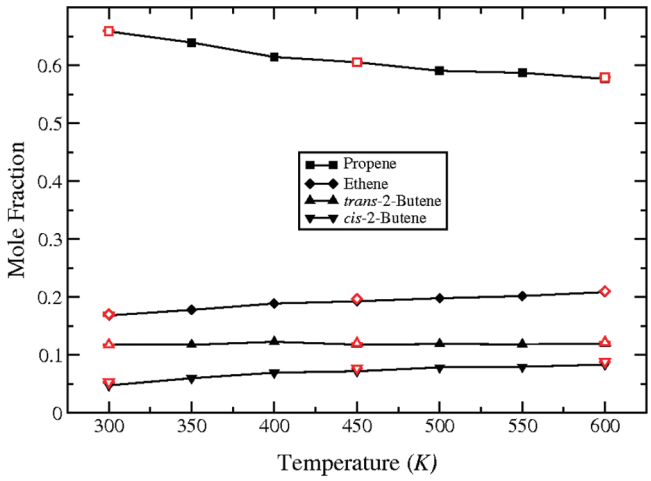

Figure 3. Equilibrium compositions for the propene metathesis reaction. Closed symbols correspond to the work of Keil et al.,[15] and open symbols correspond to the present work.

are shown in Figure 3. Results from the present work equal that of Keil and co-workers to within statistical precision. That is to say, the acceptance rule in eq 24 is consistent with the acceptance rule independently derived by Keil and co-workers. In addition, the system was simulated at 300 K using eq 25, resulting in an equilibrium mole fraction for propene of 0.89. By including the energetic penalty of creating a dihedral angle, the number of products decreased. The propene metathesis reaction at the temperatures and pressures examined in this work occurs at very dilute concentrations where one would expect mostly ideal behavior. At 300 K in an ideal gas solution, the equilibrium mole fraction of propene would be 0.657, which is very close to the results using eq 24.

Finally, the continuous fractional component method within the reaction ensemble was applied to the MTBE system. Figure 4 displays the computed equilibrium compositions using single stage insertions as well as using the CFC method. Both methods yield the same concentrations in both the condensed and gas phases. In the gas phase, though, it is unnecessary to perform gradual insertions and deletions because of the low density. Single stage reaction steps in the gas phase had an acceptance rate of ≈60%. In the liquid phase, though, single stage reaction steps had an acceptance rate <0.08%. It is for these systems, where high density causes most single stage reaction moves to be rejected, that the CFC method is expected to be most beneficial. Analysis of the efficiency of the CFC method was therefore conducted on the condensed phase MTBE synthesis reaction where the initial ratio of isobutene to methanol equaled, $r = 1.0$.

As stated in the Simulation Details Section, λ space was divided into 10 equal subsections with each given a weight, $\eta(\lambda)$, calculated during the equilibrium simulation using the Wang−Landau method.[29] These weights are inversely proportional to the free energies of the subsections, which allows the simulation to push through any free energy barrier and sample λ space equally. Figure 5 displays $-\eta$ as a function of λ for $r = 1.0$. The free energy barrier that needed to be overcome when gradually inserting a molecule was

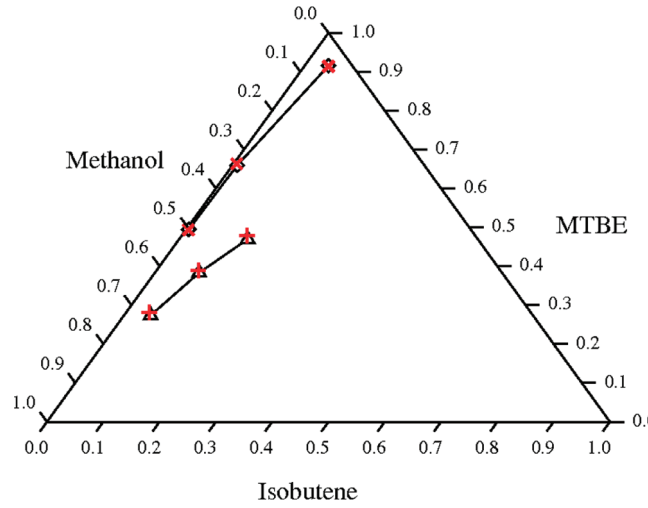

Figure 4. Triangular composition simplex for MTBE synthesis at $T = 360$ K and $P = 5$ bar. Diamonds and triangles correspond to liquid- and vapor-phase equilibrium compositions, respectively, for single stage molecule reaction moves. Plus (+) signs and × symbols correspond to vapor- and liquid-phase equilibrium compositions, respectively, for the CFC MC method.

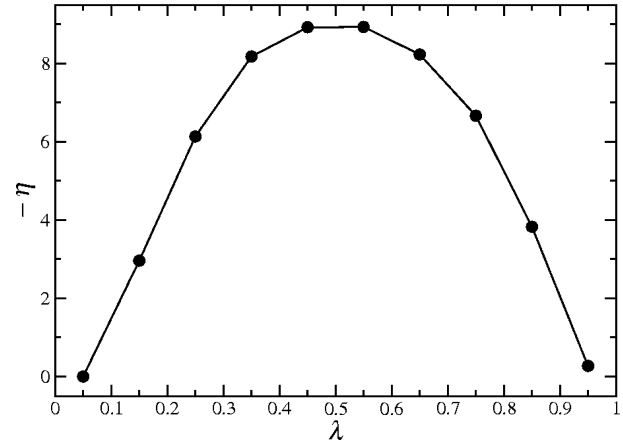

Figure 5. Inverse Wang−Landau weight for the MTBE synthesis reaction at $T = 360$ K, $P = 5$ bar, and initial isobutene to methanol mol ratio $r = 1.0$.

≈$9k_BT$, which is large enough that gradual insertion without a bias function would not be possible.

Both a CFC RxMC simulation using this weighting function and a RxMC simulation using single stage molecule insertions and deletions were run for the same amount of time. Figure 6 displays the number of isobutene molecules in the simulation box as a function of time for both methods.The averages of the CFC and the integer method were calculated to be $N_I^{avg} = 0.041 \pm 0.007$ and 0.044 ± 0.010, respectively. Overall both methods gave statistically equivalent equilibrium concentrations, yet the integer method's uncertainty was larger. This is a result of fluctuations associated with integer molecule insertions and deletions being larger than those for CFC.

While the use of the CFC method results in the same equilibrium concentration as single stage molecule insertions and deletions, the potential benefit of the method is its efficiency when insertions are difficult. The single stage

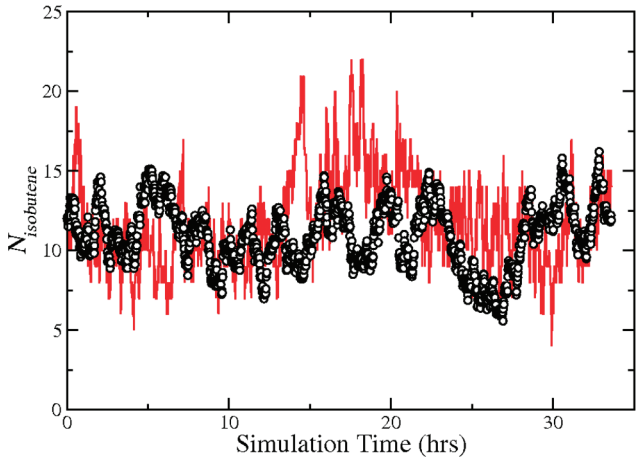

Figure 6. Number of isobutene molecules as a function of simulation time. The solid line and open symbols correspond to integer molecule insertion and deletion and CFC, respectively. For the CFC MC method $N_{\text{isobutene}} = N_{\text{isobutene}}^{\text{integer}} + \lambda$.

method achieved acceptance rates under 0.1%. Low acceptance rates mean that much of the time during simulation the system does not actually change configuration or density. The slow growth method allowed for the density to change gradually and thus more frequently. For all CFC simulations a maximum $\Delta\lambda$ of 0.3 was used. For λ moves of the first category (no additions or deletions of molecules) the acceptance rate was ≈35%. For changes in λ that resulted in new fractional molecules inserted into the system the acceptance rate was a little lower at ≈15%. These acceptance rates change the system configuration and density much more frequently than the integer insertion method, yet still may not be the best metric to show the efficiency of CFC MC. Even though reaction moves may be accepted, they may result in fluctuations about an integer molecule number, i.e., from $N_1 = 14.9 \rightarrow N_1 = 15.05 \rightarrow N_1 = 14.97$. Two accepted reaction moves of this type are not comparable to two accepted reaction moves with the integer method. Therefore whole number molecule changes within CFC MC calculations were tracked. A whole number change occurred, for example, for a system starting at $N_1 = 14.9$ only if the system changed to $N_1 < 14.0$ or $N_1 > 16.0$. Using this metric for the simulation corresponding to Figure 6, the integer method results in 4283 full molecule changes, while the CFC method results in 5083 (18.7% greater). Please note that no effort to optimize the parameters associated with the CFC method (maximum $\Delta\lambda$, number of subensembles, attempt probability for λ moves, V_{in} and $\hat{p}$ for preferential bias) has been made, which may further increase its efficiency. Also it is important to note that the increase of whole number molecule changes occurred despite changes in λ being attempted 10 times less often than in reactions using single stage molecule insertions (see Simulation Details Section).

5. Conclusions

Acceptance rules have been developed for the reaction ensemble that enables the simulation of molecules of arbitrary complexity with flexible intramolecular degrees of freedom. The acceptance rules have been developed using both a single stage transformation method as well as a "slow growth" staged deletion and insertion procedure designed to make transitions more efficient for large complex molecules. The approach was tested by simulating two systems previously examined with RxMC: MTBE synthesis and the propene metathesis reaction.

For the MTBE system, differences in composition were observed between the present work and that of Lísal et al.[20,21] It was shown that most of the discrepancies were due to a small difference in the acceptance rules used in the two studies. It is argued that the acceptance rule developed in the present work should be used when molecules with flexible intramolecular degrees of freedom are simulated.

For the propene metathesis reaction, the results obtained in the present study agree quantitatively with those of Keil and coworked.[15] Their formulation of acceptance rules within the configurational bias sampling scheme is formally identical to those developed in the present work.

The use of the slow growth continuous fractional component Monte Carlo method improved computational and sampling efficiency as compared to single stage molecule insertions and deletions. While in both cases it was possible to carry out the simulations without the use of a slow growth method, it is anticipated that for larger molecules or those in either a highly confined environment or a very dense phase, this type of slow growth approach will be essential.

Acknowledgment. The authors thank Martin Lísal and William Smith for discussions and suggestions that were critical to this work. Computational resources were provided by the University of Notre Dame Center for Research Computing. This material was financially supported by the Department of Energy (National Energy Technology Laboratory) under award number DE-FC26-07NT43091.

References

(1) Car, R.; Parrinello, M. *Phys. Rev. Lett.* **1985**, *55*, 2471–2474.

(2) Turner, C. H.; Brennan, J. K.; Lisal, M.; Smith, W. R.; Johnson, J. K.; Gubbins, K. E. *Mol. Simul.* **2008**, *34*, 119–146.

(3) Brenner, D. W. *Phys. Rev. B: Condens. Matter* **1990**, *42*, 9458–9471.

(4) Stuart, S. J.; Tutein, A. B.; Harrison, J. A. *J. Chem. Phys.* **2000**, *112*, 6472–6486.

(5) van Duin, A. C. T.; Dasgupta, S.; Lorant, F.; Goddard, W. A. *J. Phys. Chem. A* **2001**, *105*, 9396–9409.

(6) Santiso, E. E.; Gubbins, K. E. *Mol. Simul.* **2004**, *30*, 699–748.

(7) Smith, W. R.; Triska, B. *J. Chem. Phys.* **1994**, *100*, 3019–3027.

(8) Johnson, J. K.; Panagiotopoulos, A. Z.; Gubbins, K. E. *Mol. Phys.* **1994**, *81*, 717–733.

(9) Norman, G. E.; Filinov, V. S. *High Temp.* **1969**, *7*, 216–222.

(10) Turner, C. H.; Johnson, J. K.; Gubbins, K. E. *J. Chem. Phys.* **2001**, *114*, 1851–1859.

(11) Carrero-Mantilla, J.; Llano-Restrepo, M. *Fluid Phase Equilib.* **2004**, *219*, 181–193.

(12) Carrero-Mantilla, J.; Llano-Restrepo, M. *Fluid Phase Equilib.* **2006**, *242*, 189–203.

(13) Lisal, M.; Nezbeda, I.; Smith, W. R. *J. Chem. Phys.* **1999**, *110*, 8597–8604.

(14) Lisal, M.; Brennan, J. K.; Smith, W. R. *J. Chem. Phys.* **2006**, *124*, 064712.

(15) Hansen, N.; Jakobtorweihen, S.; Keil, F. J. *J. Chem. Phys.* **2005**, *122*, 164705.

(16) Jakobtorweihen, S.; Hansen, N.; Keil, F. J. *J. Chem. Phys.* **2006**, *125*, 224709.

(17) Macedonia, M. D.; Maginn, E. J. *Mol. Phys.* **1999**, *96*, 1375–1390.

(18) Vlugt, T. J. H.; Krishna, R.; Smit, B. *J. Phys. Chem. B* **1999**, *103*, 1102–1118.

(19) Martin, M. G.; Siepmann, J. I. *J. Phys. Chem. B* **1999**, *103*, 4508–4517.

(20) Lisal, M.; Smith, W. R.; Nezbeda, I. *AIChE J.* **2000**, *46*, 866–875.

(21) Lisal, M.; Smith, W. R.; Nezbeda, I. *J. Phys. Chem. B* **1999**, *103*, 10496–10505.

(22) Lisal, M.; Brennan, J. K.; Smith, W. R. *J. Chem. Phys.* **2006**, *125*, 164905.

(23) Lisal, M.; Brennan, J. K.; Smith, W. R. *J. Chem. Phys.* **2009**, *130*, 104902.

(24) Hill, T. L. *Statistical Mechanics: Principles and Selected Applications*; Dover Publications: New York, 1987.

(25) Pedley, J. *Thermodynamical Data and Structures of Organic Compounds, TRC Data Series*; Thermodynamic Research Center: College Station, TX, 1994.

(26) Chase, M. *NIST-JANAF Thermochemical Tables*, Journal of Physical and Chemical Reference Data, Monograph 9; American Physical Society: Melville, NY, 1998.

(27) Allen, M.; Tildesley, D. *Computer Simulation of Liquids*; Clarendon Press: Oxford, 1987.

(28) Shi, W.; Maginn, E. J. *J. Chem. Theory Comput.* **2007**, *3*, 1451–1463.

(29) Wang, F. G.; Landau, D. P. *Phys. Rev. Lett.* **2001**, *86*, 2050–2053.

(30) Owicki, J. C.; Scheraga, H. A. *Chem. Phys. Lett.* **1977**, *47*, 600–602.

(31) Frenkel, D.; Smit, B. *Understanding Molecular Simulation, From Algorithms to Applications*; Academic Press: New York, 2002.

(32) Martin, M. G.; Siepmann, J. I. *J. Phys. Chem. B* **1998**, *102*, 2569–2577.

(33) Wick, C. D.; Martin, M. G.; Siepmann, J. I. *J. Phys. Chem. B* **2000**, *104*, 8008–8016.

(34) Kofke, D. A. *Mol. Phys.* **2004**, *102*, 405–420.

(35) Shah, J. K.; Maginn, E. J. *J. Phys. Chem. B* **2005**, *109*, 10395–10405.

(36) Paluch, A. S.; Jayaraman, S.; Shah, J. K.; Maginn, E. J. *J. Chem. Phys.* **2010**, *133*, 124504.

CT100615J